

Dynamics of Mechanical Sliding System with Dry Friction

Dariusz Grzelczyk, Jan Awrejcewicz, Grzegorz Kudra
Department of Automation, Biomechanics and Mechatronics
Lodz University of Technology
dariusz.grzelczyk@p.lodz.pl

Abstract

In the paper we consider a four degree of freedom model of a mechanical system with dry friction, which can explain non-regular vibrations of mechanical sliding system. Stick-slip vibrations are studied for the case, where body is riding on a driving belt as a foundation that moves at a constant velocity. From a mathematical point of view, the analyzed problem is governed by a set of nonlinear ordinary second order differential equations of motion, obtained using the Lagrangian method. Numerical analysis is carried out with the qualitative and quantitative theories of nonlinear differential equations reduced to the non-dimensional form. The behavior of the mentioned system is monitored via standard phase portraits, bifurcation diagram as well as Lyapunov exponents. Some interesting numerical results (periodic, quasi-periodic, chaotic and hyper-chaotic orbits) are obtained and reported in the paper.

Keywords: friction, non-regular vibrations, chaos, hyper-chaos

1. Introduction

Friction phenomenon in many mechanical systems have the great impact on the strength of elements of these systems and their dynamics. In the scientific literature there are lots of works devoted to stick-slip vibrations in systems with dry friction. There are stick-slip induced vibrations caused by friction as a nonlinear function of the relative sliding velocity between surfaces of bodies rubbing themselves in many mechanical systems (for instance in clutches, brakes, linear sliding guide systems and others). Usually these vibrations are undesirable and even harmful. In most cases, in the scientific literature, papers from a mechanical point of view are mainly focused on dry friction stick-slip vibrations with various models of friction. As mentioned earlier there are lots of references in the scientific literature dedicated to stick-slip vibrations. Also in the last decades these kind of vibrations were the aim of research of many authors, for instance in the references [Galvanetto U., Bishop S., 1999, Guglielmino E., et al, 2004, Leine R.I., 1998]. Dry friction causing stick-slip vibrations belongs to one of the most known phenomena exhibited by mechanical systems. In general, it is a complex process and depends on different system parameters (relative velocity, normal load,

The considered planar system is in the Cartesian coordinate system with horizontal and vertical axes x and y , respectively. The first body denoted by 1 has a mass m_1 and moment of inertia about the pivot axis S equal to I . In turn, the second body denoted by 2 has mass m_2 . In our case x_1 denotes the coordinate of the body 1 in the x -direction, y_1 denotes the coordinate of the body 1 in the y -direction, φ denotes the rotation of the body 1 about the pivot axis S , while x_2 is the coordinate of the body 2 in the x -direction. The considered system is in the Earth's gravitational field with the gravity coefficient g . The presented system is characterized by lengths l_i ($i=1,2,\dots,7$), which denote distances between point S and points of fixing of springs. Moreover, the system is characterized by springs with stiffness coefficients k_{1x} , k_{2x} , k_{3y} , k_{4x} , k_{4y} , k_{5x} , k_{5y} , k_{6x} , k_{6y} , where indexes (1,2,3,4,5,6) denote numbers of springs, and indexes x and y denote the appropriate directions of acting forces produced by springs. As can be seen in figure 1, the body 2 is laying on a belt (as a foundation), which is moving with a constant velocity v_0 . Dry friction force F_{fr} occur between the body 2 and the belt, which is a nonlinear function of the relative sliding velocity $v_0 - \dot{x}_2$ of the belt and the body 2.

The equations of motion of the studied mechanical system have been derived using both the Newton-Euler method and Lagrangian method, however only a dynamic model of the system is presented obtained using Lagrangian method (the second kind Lagrange's equations)

$$\frac{d}{dt} \left(\frac{\partial T}{\partial \dot{\mathbf{q}}} \right) - \frac{\partial T}{\partial \mathbf{q}} + \frac{\partial V}{\partial \mathbf{q}} = \mathbf{Q}_n, \quad (1)$$

where: \mathbf{q} is a vector of generalized coordinates, \mathbf{Q}_n is a vector of generalized non-conservative forces acting in the system, T is a total kinetic energy, V is a total potential energy, while t is a time. Here a dot denotes differentiation with respect to time t . In our case the vector \mathbf{q} has the form $\mathbf{q} = [x_1, y_1, \varphi, x_2]^T$, while the vector \mathbf{Q}_n has the form $\mathbf{Q}_n = [0, -m_1 g, 0, F_{fr}]^T$.

The friction force F_{fr} is equal to product of the nonlinear kinetic friction coefficient $\mu_k(v_0 - \dot{x}_2)$ and the normal force N . The friction force F_{fr} strongly depends on the normal force $N = m_2 g - (k_{3y} y_1 - k_{3y} I_3 \varphi)$ pressing the body 2 to the belt. It should also be noted, that as a result of numerical simulations calculated value of the normal force N maybe greater than zero, equal to zero, or less than zero. If $N > 0$, then the friction contact between the body 2 and the belt moving at velocity v_0 occur. In turn, $N \leq 0$ means a loss of friction contact between the body

2 and the belt. For this reason, in our mathematical model we added a discontinuous step function $\mathbf{1}(N)$ describing this phenomenon, and defined as

$$\mathbf{1}(N) = \begin{cases} 1 & \text{if } N > 0 \\ 0 & \text{if } N \leq 0 \end{cases} \quad (2)$$

Finally, friction force in our model has the following form

$$F_{fr}(v_0 - \dot{x}_2, y_1, \varphi) = \mu_k (v_0 - \dot{x}_2) [m_2 g - (k_{3y} y_1 - k_{3y} l_3 \varphi)] \cdot \mathbf{1}(m_2 g - (k_{3y} y_1 - k_{3y} l_3 \varphi)). \quad (3)$$

Total kinetic energy T of the system is equal

$$T = \frac{1}{2} m_1 (\dot{x}_1^2 + \dot{y}_1^2) + \frac{1}{2} I \dot{\varphi}^2 + \frac{1}{2} m_2 \dot{x}_2^2, \quad (4)$$

and the total potential energy V of the system (for small angles φ) is

$$\begin{aligned} V = & \frac{1}{2} k_{1x} (x_1 + l_1 \varphi - x_2)^2 + \frac{1}{2} k_{2x} (x_1 + l_1 \varphi - x_2)^2 + \frac{1}{2} k_{3y} (y_1 - l_3 \varphi)^2 + \\ & + \frac{1}{2} k_{4x} (x_1 - l_2 \varphi)^2 + \frac{1}{2} k_{4y} (y_1 - l_4 \varphi)^2 + \frac{1}{2} k_{5x} (x_1 + l_5 \varphi)^2 + \frac{1}{2} k_{5y} (y_1 - l_6 \varphi)^2 + \\ & + \frac{1}{2} k_{6x} (x_1 - l_2 \varphi)^2 + \frac{1}{2} k_{6y} (y_1 + l_7 \varphi)^2. \end{aligned} \quad (5)$$

After calculating expressions $\frac{d}{dt} \left(\frac{\partial T}{\partial \dot{\mathbf{q}}} \right)$, $\frac{\partial T}{\partial \mathbf{q}}$, $\frac{\partial V}{\partial \mathbf{q}}$ and introducing into (1), finally we obtain the following equations of motion

$$\begin{cases} m_1 \ddot{x}_1 + (k_{1x} + k_{2x} + k_{4x} + k_{5x} + k_{6x}) x_1 + (k_{1x} l_1 + k_{2x} l_1 - k_{4x} l_2 + k_{5x} l_5 - k_{6x} l_2) \varphi + \\ - (k_{1x} + k_{2x}) x_2 = 0, \\ m_1 \ddot{y}_1 + (k_{3y} + k_{4y} + k_{5y} + k_{6y}) y_1 + (-k_{3y} l_3 - k_{4y} l_4 - k_{5y} l_6 + k_{6y} l_7) \varphi = -m_1 g, \\ I \ddot{\varphi} + (k_{1x} l_1 + k_{2x} l_1 - k_{4x} l_2 + k_{5x} l_5 - k_{6x} l_2) x_1 + (-k_{3y} l_3 - k_{4y} l_4 - k_{5y} l_6 + k_{6y} l_7) y_1 + \\ + (k_{1x} l_1^2 + k_{2x} l_1^2 + k_{3y} l_3^2 + k_{4x} l_2^2 + k_{4y} l_4^2 + k_{5x} l_5^2 + k_{5y} l_6^2 + k_{6x} l_2^2 + k_{6y} l_7^2) \varphi + \\ - (k_{1x} + k_{2x}) l_1 x_2 = 0, \\ m_2 \ddot{x}_2 - (k_{1x} + k_{2x}) x_1 - (k_{1x} + k_{2x}) l_1 \varphi + (k_{1x} + k_{2x}) x_2 = \\ \mu_k (v_0 - \dot{x}_2) [m_2 g - (k_{3y} y_1 - k_{3y} l_3 \varphi)] \cdot \mathbf{1}(m_2 g - (k_{3y} y_1 - k_{3y} l_3 \varphi)). \end{cases} \quad (6)$$

3. Non-dimensional form

Let us introduce non-dimensional time $\tau = t / \sqrt{m_1 / (k_{1x} + k_{2x})}$, non-dimensional coordinates $X_1 = x_1 / l_1$, $Y_1 = y_1 / l_1$ and $X_2 = x_2 / l_1$, non-dimensional parameters

$$\begin{aligned}
a_1 &= \frac{m_2}{m_1} \left(1 + \frac{k_{4x} + k_{5x} + k_{6x}}{k_{1x} + k_{2x}} \right), \quad a_2 = \frac{m_2}{m_1} \left(1 + \frac{-k_{4x}l_2 + k_{5x}l_5 - k_{6x}l_2}{(k_{1x} + k_{2x})l_1} \right), \quad a_3 = \frac{m_2}{m_1}, \\
b_1 &= \frac{m_2}{m_1} \frac{k_{3y} + k_{4y} + k_{5y} + k_{6y}}{k_{1x} + k_{2x}}, \quad b_2 = \frac{m_2}{m_1} \frac{k_{3y}l_3 + k_{4y}l_4 + k_{5y}l_6 - k_{6y}l_7}{(k_{1x} + k_{2x})l_1}, \\
c_1 &= \frac{m_2 l_1 (k_{1x}l_1 + k_{2x}l_1 - k_{4x}l_2 + k_{5x}l_5 - k_{6x}l_2)}{(k_{1x} + k_{2x})l}, \\
c_2 &= \frac{m_2 l_1 (k_{3y}l_3 + k_{4y}l_4 + k_{5y}l_6 - k_{6y}l_7)}{(k_{1x} + k_{2x})l}, \\
c_3 &= \frac{m_2 (k_{1x}l_1^2 + k_{2x}l_1^2 + k_{3y}l_3^2 + k_{4x}l_2^2 + k_{4y}l_4^2 + k_{5x}l_5^2 + k_{5y}l_6^2 + k_{6x}l_2^2 + k_{6y}l_7^2)}{(k_{1x} + k_{2x})l}, \\
c_4 &= \frac{m_2 l_1^2}{l}, \quad e_1 = \frac{k_{3y}}{k_{1x} + k_{2x}}, \quad e_2 = \frac{l_3}{l_1} \frac{k_{3y}}{k_{1x} + k_{2x}}, \quad f_g = \frac{m_2 g}{(k_{1x} + k_{2x})l_1}, \quad V_0 = \frac{v_0}{l_1} \sqrt{\frac{m_2}{k_{1x} + k_{2x}}},
\end{aligned}$$

and non-dimensional functions

$$\begin{aligned}
\mu_k \left(\frac{l_1}{\sqrt{m_2/(k_{1x} + k_{2x})}} V_0 - \frac{l_1}{\sqrt{m_2/(k_{1x} + k_{2x})}} \frac{dX_2}{d\tau} \right) &= f_k(V_0 - \dot{X}_2), \\
\mathbf{1}((k_{1x} + k_{2x})l_1 f_g - (k_{1x} + k_{2x})l_1 (e_1 Y_1 - e_2 \varphi)) &= \mathbf{1}(f_g - (e_1 Y_1 - e_2 \varphi)),
\end{aligned}$$

where now dot denotes differentiation with respect to non-dimensional time τ . Then equations of motion (6) can be reduced to the following non-dimensional form

$$\begin{cases}
\ddot{X}_1 + a_1 X_1 + a_2 \varphi - a_3 X_2 = 0, \\
\ddot{Y}_1 + b_1 Y_1 - b_2 \varphi = -f_g, \\
\ddot{\varphi} + c_1 X_1 - c_2 Y_1 + c_3 \varphi - c_4 X_2 = 0, \\
\ddot{X}_2 - X_1 - \varphi + X_2 = \\
= f_k(V_0 - \dot{X}_2)[f_g - (e_1 Y_1 - e_2 \varphi)] \cdot \mathbf{1}(f_g - (e_1 Y_1 - e_2 \varphi)).
\end{cases} \quad (7)$$

4. Numerical computational methods

Numerical calculations were performed via the fourth order Runge-Kutta method with constant time step $h=0.001$ and zero initial conditions. In order to implement the computer algorithm, four second order differential equations of motion (7) are write in the form of eight first order differential equations taking $\dot{X}_1 = V_1$, $\dot{Y}_1 = Z_1$, $\dot{\varphi} = \omega$ and $\dot{X}_2 = V_2$. In this paper kinetic friction function $f_k(V_0 - V_2)$ is described by the Stribeck curve. Since classical signum function is

non-smooth, in our studies we approximate the mentioned function by hyperbolic tangent function with numerical control parameter ε

$$f_k(V_0 - V_2) = \mu_0 \tanh\left(\frac{V_0 - V_2}{\varepsilon}\right) - \alpha(V_0 - V_2) + \beta(V_0 - V_2)^3. \quad (8)$$

Similarly, since function $\mathbf{1}(f_g - (e_1 Y_1 - e_2 \varphi))$ is also non-smooth, in our calculations we replaced this function using smooth function $f_n(f_g - (e_1 Y_1 - e_2 \varphi))$ defined as follows

$$f_n(f_g - (e_1 Y_1 - e_2 \varphi)) = \left[\tanh\left(\frac{f_g - (e_1 Y_1 - e_2 \varphi)}{\varepsilon}\right) \right]^3 \cdot \mathbf{1}(f_g - (e_1 Y_1 - e_2 \varphi)), \quad (9)$$

with the same as earlier ε control parameter.

Non-dimensional friction model parameters estimated and taken from the references [Awrejcewicz J., 1981, Awrejcewicz J., Grzelczyk D., 2013] and used in our calculations are $\mu_0 = 0.8$, $\alpha = 15.59$, $\beta = 4252.12$, whereas $\varepsilon = 10^{-4}$. Dimensional parameters characterized the considered mechanical system have also been taken from the same references. Based on the mentioned dimensional values and previously determined relationships, numerical calculations have been carried out for the following non-dimensional parameters: $a_1 = 0.07836$, $a_2 = 0.03344$, $a_3 = 0.04058$, $b_1 = 0.09375$, $b_2 = 0.03314$, $c_1 = 0.02689$, $c_2 = 0.02666$, $c_3 = 0.06181$, $c_4 = 0.03264$, $f_g = 0.00529$, $e_1 = 1.37931$, $e_2 = 0.47237$.

In this paper numerical simulations were carried out for one presented above set of system parameters. The behavior of the mentioned system was monitored via phase portraits, detecting periodic and chaotic dynamics. Moreover, a good and commonly used tool for the detection of periodic and chaotic dynamics in nonlinear dynamical systems are Lyapunov exponents. However, the methods usually used to compute the Lyapunov exponents require smooth vector fields as a necessary condition. In classical signum model friction force is non-continuous function of relative velocity and therefore a continuous and smooth function $f_k(V_0 - V_2)$ is used in our paper (also $f_n(f_g - (e_1 Y_1 - e_2 \varphi))$), which does not possess this disadvantage. For this reason they can be used during analysis of the systems, where the Lyapunov exponents are computed by the standard procedures [Awrejcewicz J., Pyryev Yu., 2006, Awrejcewicz J., et al., 2008, Kuznecov S.P., 2001]. Note only, that while computing Lyapunov exponents, besides eight first order differential equations also eight additional systems of equations ($n = 1, 2, 3, \dots, 8$) with respect to perturbations should be solved. Finally, seventy two equations are solved. The obtained equations can be solved via standard the fourth order Runge-Kutta method, as well as the Gram-Schmidt orthonormalization

technique, for instance applied in [Awrejcewicz J., Pyryev Yu., 2006, Awrejcewicz J., et al., 2008, Kuznecov S.P., 2001].

5. Numerical results

Fig. 2 shows the phase trajectories of the system starting from zero initial conditions for $V_0 = 0.002$ and $V_0 = 0.01$. The trajectories are shown in the time interval $\tau \in [10000, 12000]$.

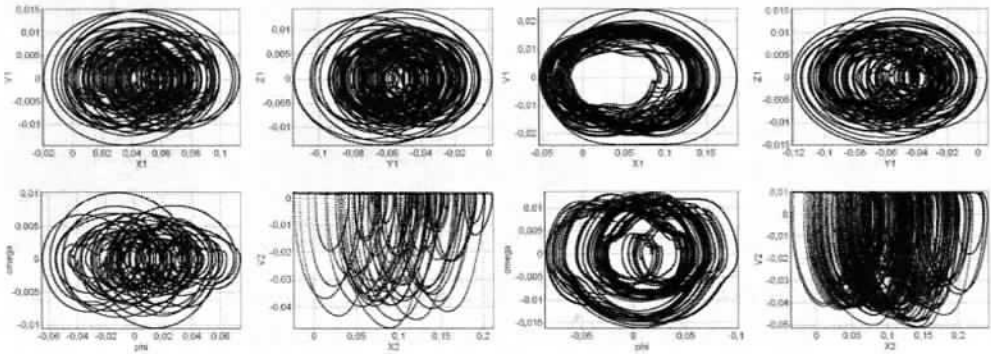


Fig. 2. Trajectories of the system for $V_0 = 0.002$ (on the left) and $V_0 = 0.01$ (on the right) in the time interval $\tau \in [10000, 12000]$.

The obtained results indicate an irregular dynamics of the considered mechanical system. Numerical simulations for a given value of the parameter V_0 carried out for longer periods of time also did not detect the periodic orbits. However, the different character of the motion has been detected for larger values of the parameter V_0 .

Fig. 3 show two chosen interesting periodic solutions for the values of the parameter V_0 equal to 0.015 and 0.032, respectively.

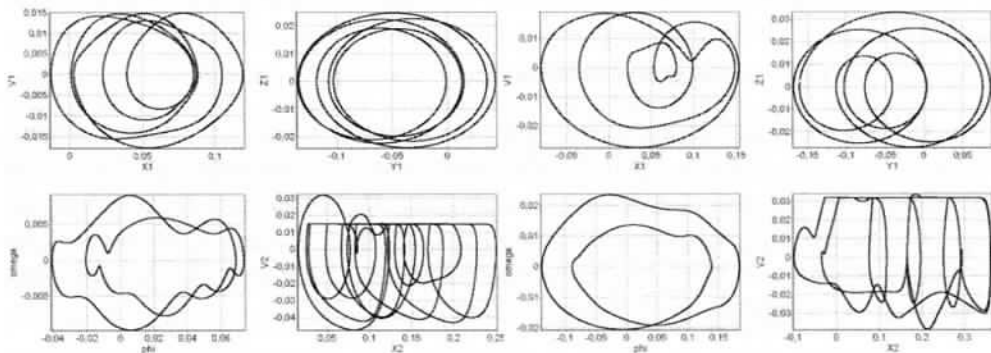


Fig. 3. Periodic orbits for $V_0 = 0.015$ (on the left) and $V_0 = 0.032$ (on the right).

Another character of motion has been detected for larger value of V_0 parameter. During simulation (here for $V_0 = 0.05$), after a transitional period, the system goes to steady state (fixed point), as can be shown in Fig. 4.

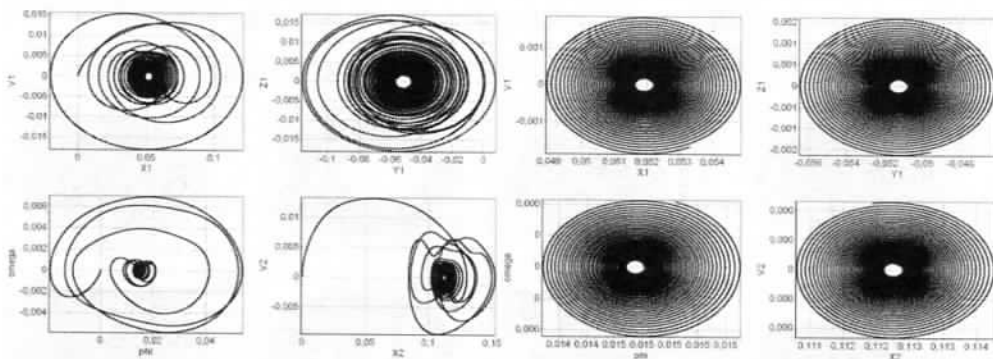


Fig. 4. Trajectories of the system for $V_0 = 0.05$ in the time interval $\tau \in [0, 1000]$ (on the left) and in the time interval $\tau \in [1000, 2000]$ (on the right).

For a more complete qualitative analysis of system dynamics bifurcational diagram has been performed with a V_0 as a control parameter and shown in Fig. 5.

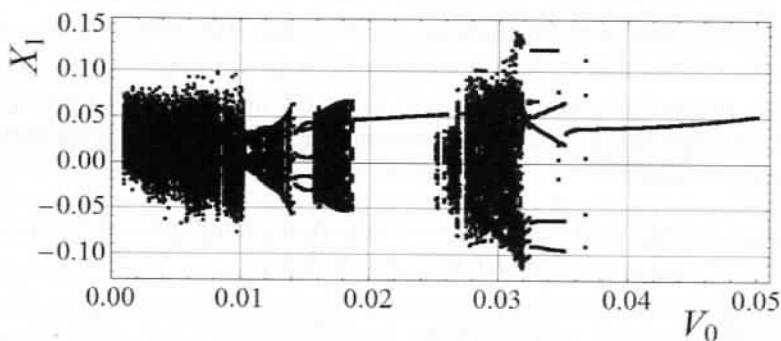


Fig. 5. Bifurcational diagram with V_0 as a control parameter.

The presented bifurcational diagram consists of 400 Poincaré sections defined as $V_1 = 0$ (rising). Each the Poincaré section is computed by the use of simulation starting from zero initial conditions. Then the first 1000 points are ignored and last 150 ones are presented in the diagram. Moreover, we present the Table 1, which contains Lyapunov exponents corresponding to the solutions presented on the bifurcational diagram in Fig. 5.

Table 1. Lyapunov exponents corresponding to the solutions presented in Fig. 5.

V_0	λ_1	λ_2	λ_3	λ_4	λ_5	λ_6	λ_7	λ_8
0.001	0.0174	0.0070	0.0020	0.0007	0.0000	-0.0007	-0.0044	-44.79
0.002	0.0214	0.0081	0.0028	0.0006	0.0000	-0.0014	-0.0010	-43.97
0.004	0.0161	0.0054	0.0014	0.0001	-0.0021	-0.0086	-0.0324	-43.11
0.005	0.0000	-0.0024	-0.0025	-0.0028	-0.0031	-0.0118	-0.0121	-38.59
0.01	0.0060	0.0012	0.0000	-0.0021	-0.0051	-0.0091	-0.0193	-36.20
0.015	0.0000	-0.0012	-0.0039	-0.0041	-0.0164	-0.0168	-0.0416	-28.03
0.02	0.0000	-0.0013	-0.0013	-0.0095	-0.0102	-0.0240	-0.0246	-29.77
0.025	0.0000	-0.0027	-0.0027	-0.0033	-0.0082	-0.0210	-0.1094	-16.15
0.03	0.00000	-0.00003	-0.00238	-0.01311	-0.01674	-0.03976	-0.15922	-13.035
0.032	0.0000	-0.0010	-0.0045	-0.078	-0.0250	-0.0272	-0.1146	-10.07
0.04	-0.0011	-0.0011	-0.0067	-0.0067	-0.0148	-0.0149	-0.266	-0.266
0.05	-0.0035	-0.0035	-0.0188	-0.0188	-0.0638	-0.0638	-0.899	-0.899

The Lyapunov exponents for chosen V_0 parameters have been computed using period ΔT of the Gram-Schmidt reorthonormalization equal to 0.5 ($\Delta T = 0.5$), along the trajectory of length 10^5 (for $V_0 = 0.03$ exceptionally $5 \cdot 10^5$) and after ignoring the initial motion, starting from the zero initial conditions. Among the selected parameter values of V_0 chaotic behaviors are detected for V_0 equal to 0.001, 0.002, 0.004, 0.01, while periodic behaviors are detected for V_0 equal to 0.005, 0.015, 0.02, 0.025, 0.03, 0.032. For $V_0 = 0.04$ and $V_0 = 0.05$ trajectories goes to a fixed point. The obtained values of Lyapunov exponents confirm the periodic and chaotic behavior of the system depending on the selected parameter V_0 .

6. Summary and conclusions

In this paper mathematical modeling of the 4-DOF mechanical linear sliding guideways system with dry friction is shown. The analyzed system from mathematical point of view is presented as a nonlinear equations of motion obtained from second kind Lagrange's equations. Numerical analysis of the system in non-dimensional form were carried out for one set of system parameters and various V_0 control parameter. Some interesting behaviors of the system are detected using standard phase portraits. For a more complete qualitative analysis of system dynamics, bifurcational diagram has been performed with a V_0 as a control parameter. Moreover, Lyapunov exponents corresponding to the solutions presented on the mentioned bifurcational diagram have been computed and analysed. The obtained Lyapunov exponents confirm periodic and chaotic behavior of the system obtained using phase trajectories as well as bifurcational diagram. Presented results show interesting solutions, including periodic, quasi-periodic, chaotic and hyper-chaotic orbits. Moreover, for relatively large value of control parameter V_0 trajectories of the system goes to a fixed point. On the other hand, as can be seen in the table 1, for relatively small value of parameter V_0 we obtain hyper-chaotic solutions with two, three or four positive Lyapunov exponents.

Acknowledgments

The work has been supported by the National Science Foundation of Poland under the grant MAESTRO2 No. 2012/04/A/ST8/00738 for years 2012-2016.

References:

- Andersson S., Soderberg A., Bjorklund S.:** Friction models for sliding dry, boundary and mixed lubricated contacts. *Tribology International* 40, 2007, 580-587.
- Awrejcewicz J.:** Analysis of stick-slip vibrations of mechanical systems caused by nonlinear friction. *Lodz University of Technology*, 1981, 180 pages (in Polish).
- Awrejcewicz J., Lamarque C.-H.:** Bifurcation and chaos in nonsmooth mechanical systems. Vol. 45 Series A, *World Scientific*, New Jersey, London, Singapore, 2003.
- Awrejcewicz J., Olejnik P.:** Analysis of dynamics systems with various friction laws. *Applied Mechanics Reviews* 58(6), 2005, 389-411.
- Awrejcewicz J., Pyryev Yu.:** Regular and chaotic motion of a bush-shaft system with tribological processes. *Mathematical Problems in Engineering*, 2006, (DOI: 10.1155/MPE/2006/86594).
- Awrejcewicz J., Grzelczyk D., Pyryev Yu.:** A novel dry friction modeling and its impact on differential equations computation and Lyapunov exponents estimation. *Journal of Vibroengineering* 10(4), 2008, 475-482.
- Awrejcewicz J., Grzelczyk D.:** Non-regular dynamics of the 4-DOF mechanical linear sliding guideways system with dry friction. *Dynamical Systems - Applications*, Eds. J. Awrejcewicz, M. Kaźmierczak, P. Olejnik, J. Mrozowski, *TU of Lodz Press*, 2013, 483-496 (ISBN 978-83-7283-589-5).
- Galvanetto U., Bishop S.:** Dynamics of a simple damped oscillator undergoing stick-slip vibrations. *Meccanica* 34, 1999, 337-347.
- Guglielmino E., Edge K.A., Ghigliazza R.:** On the control of the friction force. *Meccanica* 39, 2004, 395-406.
- Hinrichs N., Oestreich M., Popp K.:** Dynamics oscillators with impact and friction. *Chaos, Solitons and Fractals* 8(4), 1997, 535-558.
- Ibrahim R. A.:** Friction-induced vibration, chatter, sequel, and chaos. Part I: Mechanics of contact and friction. *Applied Mechanics Reviews* 47(7), 1994, 209-226.
- Kuznecov S.P.:** Dynamical chaos. Moskva *Fizmatlit*, 2001 (in Russian).
- Leine R.I., Van Campen D.H., De Kraker A., Van den Steen:** Stick-slip vibrations induced by alternate friction models. *Nonlinear Dynamics* 16(1), 1998, 41-54.
- Martins J. A. C., Oden J. T., Simoes F. M. F.:** A study of static and kinetic friction. *International Journal of Engineering Science* 28(1), 1990, 29-92.
- Valcovici V., Balan S.T., Voinea R.:** Mecanica teoretica. *Editura Tehnica*, Bucuresti, 1963.